Phase Equilibria of Methane and Carbon Dioxide Clathrate Hydrates in the Presence of Aqueous Solutions of Tributylmethylphosphonium Methylsulfate Ionic Liquid

ARTICLE *in* JOURNAL OF CHEMICAL & ENGINEERING DATA · SEPTEMBER 2011

Impact Factor: 2.04 · DOI: 10.1021/je200462q

JOURNAL OF CHEMICAL & ENGINEERING DATA

ARTICLE

pubs.acs.org/jced

Phase Equilibria of Methane and Carbon Dioxide Clathrate Hydrates in the Presence of Aqueous Solutions of Tributylmethylphosphonium Methylsulfate Ionic Liquid

Kaniki Tumba, Prashant Reddy, Paramespri Naidoo, and Deresh Ramjugernath

Thermodynamics Research Unit, School of Chemical Engineering, University of KwaZulu-Natal, Howard College Campus, King George V Avenue, Durban 4041, South Africa

Ali Eslamimanesh, Amir H. Mohammadi,* and Dominique Richon

MINES ParisTech, CEP/TEP, Centre Énergétique et Procédés, 35 Rue Saint Honoré, 77305 Fontainebleau, France

ABSTRACT: The effect of a tributylmethylphosphonium methylsulfate ionic liquid (IL) aqueous solution on the equilibrium conditions of carbon dioxide and methane clathrate hydrates was studied. An isochoric pressure-search method was used to measure the hydrate dissociation conditions for the carbon dioxide + tributylmethylphosphonium methylsulfate + water and methane + tributylmethylphosphonium methylsulfate + water systems in the temperature ranges of (273.5 to 282.2) K and (273.3 to 288.5) K, and pressures up to (4.35 and 14.77) MPa, respectively. The concentrations of tributylmethylphosphonium methylsulfate in the aqueous solutions were 0, 0.2611, and 0.5007 mass fractions. The good agreement between our experimental hydrate dissociation data in the absence of tributylmethylphosphonium methylsulfate with selected literature experimental data demonstrates the reliability of the experimental method used in this work. The comparison between the hydrate dissociation conditions in the presence and absence of tributylmethylphosphonium methylsulfate shows that the IL has an inhibition effect on carbon dioxide and methane clathrate hydrate formation. Furthermore, a thermodynamic model, developed based on van der Waals−Platteeuw solid solution theory accompanied with the Peng−Robinson equation of state (PR-EoS) and the nonrandom two-liquid (NRTL) activity model, was successfully applied to represent/predict the obtained experimental data.

1. INTRODUCTION

Clathrate hydrates, or gas hydrates, are ice-like crystalline solids consisting of small molecules (guests), which are typically low molecular diameter gas molecules and organic compounds. These are encapsulated into cage-like structures made of hydrogen-bonded water molecules that are generally stable at high pressures and low temperatures.[1] The common gas hydrate crystalline structures are structure I (sI), structure II (sII), and structure H (sH), where each structure is composed of a characteristic number of cavities formed by water molecules.[1] The size of a molecule which is able to enter a cavity should be smaller than a certain value.[1] In the case of sH structures, large guest molecules can enter inside only a limited number of large cavities requiring small "help gas" molecules, like methane, and so forth to stabilize hydrate crystals.[1]

Formation of gas hydrates is a serious problem in hydrocarbon production, transportation, and processing as it can give rise to equipment blockage, operational problems, and safety concerns.[1] To avoid the formation of gas hydrates, aqueous solutions of organic inhibitors like methanol or ethylene glycol are normally used, which shift hydrate equilibrium conditions to higher pressures and/or lower temperatures.[1]

On the other hand, it is worth it to note that a number of positive applications of clathrate hydrates have been extensively proposed through the use of gas hydrate formation technology, for example, in the refrigeration and air conditioning industry,[1−17] water desalination/treatment,[18,19] and the food industry, especially for producing fruit concentrates[20,21] and as a potential medium for gas separation, storage, and transportation.[22−40]

Even if the objective of this paper is to describe the inhibition ability of an ionic liquid, the reader must be informed that different chemical compounds, added to the system, may behave either as inhibitors or promoters. As a matter of fact, it is known that the pressure required for gas hydrate formation especially for separation processes is generally high.[1,28−30] The judicious addition of some organic compounds, called "water-soluble" or "water-insoluble" hydrate promoters, lowers the hydrate equilibrium pressure at a given temperature or raises the hydrate equilibrium temperature at a given pressure.[1,31−34] Economical, safety, and environmental aspects are important in selecting the aforementioned water-soluble or water insoluble compounds.[1,26] Some tetra-alkylammonium halides, which are water-soluble, such as tetrabutyl ammonium bromide (TBAB), tetrabutyl ammonium fluoride (TBAF), tetrabutyl ammonium chloride (TBAC), and so forth, and some tetra-alkylphosphonium halides like tetrabutylphosphonium bromide (TBPB) have already been proposed as promoters of gas hydrates.[35−40] Because of the nature of their constitution, these promoters are considered as kinds of ionic liquids (ILs). Room-temperature ILs are organic salts that are generally liquid at room temperatures.[41−43] They

Received: May 11, 2011
Accepted: July 1, 2011
Published: August 15, 2011

are normally composed of a large organic cation and organic or inorganic anions.[41−43] The applications of ILs have generated a large number of interests in the past decade.[41−43] This is mainly because of their tunable properties that can be controlled by a judicious combination of cations and anions.[41−43] This phenomenon allows researchers to design specific solvents for the development of more efficient processes and products.[41−43] Having a negligible vapor pressure, no flammability, good thermal stability, a wide liquid range, and electrical conductivity, and so forth are a few of the attributes, among others, that have made ILs an active hub of research.[41−43]

To the best of our knowledge, there is limited information available in open literature on the effects of ILs on gas hydrate formation. Thus far, Chen et al.[44] have identified 1-butyl-3-methylimidazolium tetrafluoroborate as a reasonable thermodynamic inhibitor for carbon dioxide hydrate formation. The great interest of their findings lies in the fact that ILs, generally viewed as safe and eco-friendly solvents, would be more attractive than the commonly used inhibitors which pose a number of environmental concerns.[41−43] However, this is not a universal statement as some ILs are not as eco-friendly as they would be desired to be. Some (containing fluorinated anions) undergo thermal decomposition to release HF. Indeed, the IL used here is water-endangering, and so containment and closed-loop recycling is important.

In similar studies,[45,46] it was found that some imidazolium-based ILs do not only act as thermodynamic inhibitors but can be considered as kinetic inhibitors for the methane + water hydrate forming system. The studied ILs have contained the following cations: 1-ethyl-3-methylimidazolium, 1-propyl-3-methylimidazolium, and 1-butyl-3-methylimidazolium while the anions have included tetrafluoroborate, dicyanamide, trifluoromethanesulfonate, ethylsulfate, chloride, bromide, and iodide. Moreover, Li et al.[47] reported equilibrium data for the methane hydrate in the presence of five different ILs with a chloride anion: 1,3-dimethylimidazolium, 1-ethyl-3-methyl-imidazolium, 1-hydroxyethyl-3-methylimidazolium, tetramethylammonium, and hydroxyethyltrimethylammonium. Recently, the application of gas hydrate formation phenomenon for the separation of ILs from aqueous solutions has been investigated by Peng and co-workers.[48]

Almost all previous publications have focused on the effects of imidazolium and ammonium-based ILs on gas hydrate formation processes. In this communication, the effect of a phosphonium-based IL, namely, as tributylmethylphosphonium methylsulfate or $[3C_4C_1P][MeSO_4]$, on equilibrium conditions of methane and carbon dioxide clathrate hydrates is investigated. We report experimental hydrate dissociation conditions for the carbon dioxide + tributylmethylphosphonium methylsulfate + water and methane + tributylmethylphosphonium methylsulfate + water systems in the temperature ranges of (273.5 to 282.2) K and (273.3 to 288.5) K, respectively, and pressures up to (4.35 and 14.77) MPa, respectively. The concentrations of tributylmethylphosphonium methylsulfate in water were 0, 0.2611, and 0.5007 mass fractions. There has only been one thermodynamic study on the studied IL available in the literature.[49] The obtained results clarify the inhibition effects of the investigated IL. Furthermore, a thermodynamic model is presented for the representation/prediction of the experimental data obtained in this study.

Table 1. Purities and Suppliers of Materials[a]

material	supplier	purity
methane	AFROX	0.995 (mole fraction)
carbon dioxide	AFROX	0.9999 (mole fraction)
tributylmethylphosphonium methylsulfate	Solvent Innovation	>0.98 (NMR)[b]

[a] Ultrapure Millipore Q water was used in all experiments. [b] Water content of less than 33.0 ppm.

2. EXPERIMENTAL SECTION

2.1. Materials. Table 1 reports the purities and suppliers of the chemicals used in this work. The IL was purified by subjecting the liquid to a low-pressure vacuum (10^{-4} Torr) for 6 h along with heating at 353.15 K to remove any traces of volatile contaminants including water. Aqueous solutions were prepared with a gravimetric method using an accurate analytical balance (Ohaus Adventurer balance, model no. AV 114, uncertainty in grams:

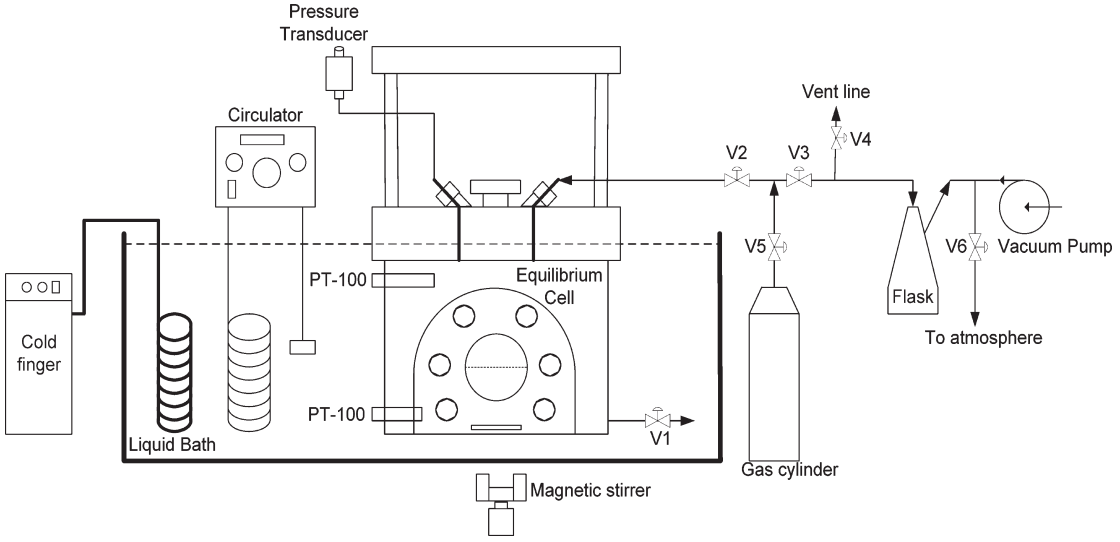

Figure 1. Schematic diagram of the apparatus used in this work. V, valve; PT, platinum probe.

Table 2. Experimental Dissociation Conditions of Clathrate Hydrates for the Carbon Dioxide + $[3C_4C_1P][MeSO_4]$ + Water and Methane + $[3C_4C_1P][MeSO_4]$ + Water Systems

0.0000[a] m[b]		0.2611 m		0.5007 m	
T[c]/K	p[d]/MPa	T/K	p[d]/MPa	T/K	p/MPa
Carbon Dioxide + $[3C_4C_1P][MeSO_4]$ + Water					
275.5[e]	1.65[f]	274.4	1.76	273.5	2.15
276.2	1.78	276.8	2.37	274	2.59
277.9	2.19	277.9	2.83	275.6	3.14
279.3	2.61	279.2	3.44	276.5	3.61
281.3	3.4	280.6	4.2	277	3.75
282.2	3.88	281.4	4.35	277.3	3.98
Methane + $[3C_4C_1P][MeSO_4]$ + Water					
277.3	3.88	275.3	4.09	273.3	4.13
283.9	7.77	278	5.46	274.6	4.90
284.8	8.64	281.5	7.51	277	6.56
284.9	8.68	283.2	9.47	278.6	8.44
287.5	11.65	285.4	12.27	280.5	10.10
288.5	13.16	287.1	14.77	282.4	14.52

[a] The interval of the confidence for estimating the uncertainties is considered to be 0.95. Therefore, the expanded uncertainties (U_c) in the reported mass fractions are ± 0.0002. [b] Mass fraction of IL. [c] Temperature. [d] Pressure. [e] The interval of the confidence for estimating the uncertainties is considered to be 0.95. Therefore, the expanded uncertainties (U_c) in the reported temperatures are ± 0.2 K. [f] The interval of the confidence for estimating the uncertainties is considered to be 0.95. Therefore, the expanded uncertainties (U_c) in the reported pressures are ± 0.01 MPa.

0.00005 g). Consequently, uncertainties on the basis of mole fraction are estimated to be below 0.01.

2.2. Experimental Apparatus. Figure 1 shows a schematic diagram of the apparatus used in this work. The main part of the apparatus is a stainless steel cylindrical cell, which can withstand pressures up to 20 MPa. The volume of the cell is approximately 60 cm^3. A magnetically coupled stirrer, incorporating rare earth magnets, was installed in the vessel. Two platinum resistance thermometers (Pt100) were used to measure temperatures and were checked for agreement within the temperature measurement uncertainty, which is estimated to be less than 0.1 K. The calibrations of the thermometers were performed against a 25 Ω reference platinum resistance thermometer (WIKA digital thermometer calibration standard, model no. CTH 6500, accuracy: ± 0.03 %). The pressure in the vessel was measured with a WIKA pressure transducer for pressures up to 20 MPa. The pressure measurement uncertainty is estimated to be less than 5 kPa, as a result of calibration against a dead weight balance.

2.3. Experimental Method. The dissociation conditions were measured with an isochoric pressure search method.[28,29,50−52] As implemented by Ohmura and coworkers,[51] the vessel containing aqueous solution (approximately 40 % by volume of the vessel was filled with aqueous solution) was immersed into the temperature-controlled bath, and the gas was supplied from a cylinder through a pressure-regulating valve into the vessel. The vessel was evacuated (down to 0.8 kPa) before the introduction of any aqueous solution/gas. After obtaining temperature and pressure stability (far enough from the hydrate formation region), the valve in the line connecting the vessel and the cylinder was closed. Subsequently, the system temperature was slowly decreased to form the hydrate, while the hydrate formation in the vessel was detected by pressure drop. The temperature was then increased with steps of 0.1 K.[28,29,50−52] At every temperature step, the temperature was kept constant with sufficient time to achieve an equilibrium state in the vessel.[28,29,50−52] In this way, a pressure−temperature diagram was obtained for each experimental run, from which we determined the hydrate dissociation point.[28,29,50−52] If the temperature is increased in the hydrate-forming region,

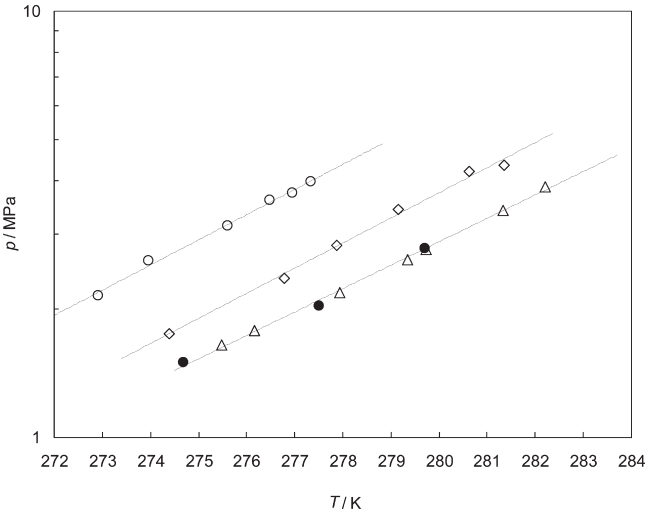

Figure 2. Dissociation conditions of clathrate hydrates for the carbon dioxide + $[3C_4C_1P][MeSO_4]$ + water systems. p = pressure; T = temperature. Symbols represent experimental data and curves (lines) represent the best fits to experimental data. ●, CO_2 + water system, literature;[68] △, CO_2 + water system, this work; ◇, CO_2 + IL + water system (0.2611 mass fraction IL), this work; ○, CO_2 + IL + water system (0.5007 mass fraction IL), this work.

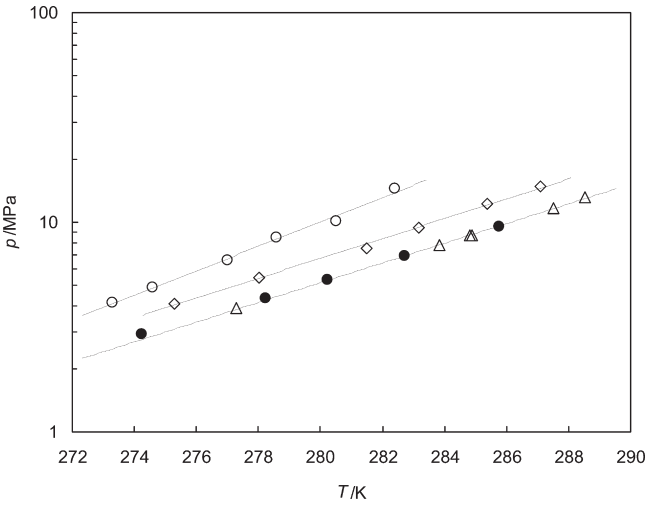

Figure 3. Dissociation conditions of clathrate hydrates for the methane + $[3C_4C_1P][MeSO_4]$ + water systems. p = pressure; T = temperature. Symbols represent experimental data, and curves (lines) represent the best fits to experimental data. ●, methane + water system, literature;[69] △, methane + water system, this work; ◇, methane + IL + water system (0.2611 mass fraction IL), this work; ○, methane + IL + water system (0.5007 mass fraction IL), this work.

Table 3. Type of Inhibitor and the Constants Required to Determine Hydrate Suppression Temperature in eq 16[70]

inhibitor	C'_1	C'_2	C'_3	C'_4	C'_5	C'_6
methanol	$4.780 \cdot 10^{-1}$	$7.170 \cdot 10^{-3}$	$-1.440 \cdot 10^{-5}$	$2.947 \cdot 10^{-2}$	$5.960 \cdot 10^{-1}$	$3.10 \cdot 10^{-5}$
ethane-1,2-diol	$3.893 \cdot 10^{1}$	$-5.220 \cdot 10^{-1}$	$1.767 \cdot 10^{-2}$	$3.503 \cdot 10^{-4}$	$5.083 \cdot 10^{-3}$	$2.65 \cdot 10^{-5}$
sodium chloride	$3.534 \cdot 10^{-1}$	$1.375 \cdot 10^{-3}$	$2.433 \cdot 10^{-4}$	$4.056 \cdot 10^{-2}$	$7.994 \cdot 10^{-1}$	$2.25 \cdot 10^{-5}$
potassium chloride	$3.050 \cdot 10^{-1}$	$6.770 \cdot 10^{-4}$	$8.096 \cdot 10^{-5}$	$3.858 \cdot 10^{-2}$	$7.140 \cdot 10^{-1}$	$2.20 \cdot 10^{-5}$
calcium dichloride	$1.940 \cdot 10^{-1}$	$7.580 \cdot 10^{-3}$	$1.953 \cdot 10^{-4}$	$4.253 \cdot 10^{-2}$	$1.023 \cdot 10$	$2.80 \cdot 10^{-5}$

hydrate crystals partially dissociate, thereby substantially increasing the pressure.[28−30,50−52] If the temperature is increased outside the hydrate region, only a smaller increase in the pressure is observed as a result of the temperature change of the fluids in the vessel.[28−30,50−52] The point at which the slope of pressure−temperature data plots changes sharply is, consequently, considered to be the point at which all hydrate crystals have dissociated, and therefore this is reported as the dissociation point.[28,29,50−52]

3. THERMODYNAMIC MODEL

The (liquid water-hydrate-gas/vapor) equilibrium of a system can be calculated by equating the fugacities of water in the liquid water phase, f_w^L, and in the hydrate phase, f_w^H, ignoring the water content of the gas/vapor phase.[53,54]

$$f_w^L = f_w^H \tag{1}$$

The fugacity of water in the hydrate phase, f_w^H, is related to the chemical potential difference of water in the filled and empty hydrate cage by the following expression:[1,53,54]

$$f_w^H = f_w^{MT} \exp \frac{\mu_w^H - \mu_w^{MT}}{RT} \tag{2}$$

where f_w^{MT} is the fugacity of water in the hypothetical empty hydrate phase and $\mu_w^H - \mu_w^{MT}$ represents the chemical potential difference of water in the filled (μ_w^H) and empty (μ_w^{MT}) hydrate. R and T stand for the universal gas constant and temperature, respectively.

The solid solution theory of van der Waals−Platteeuw[55] can be employed for calculating $(\mu_w^H - \mu_w^{MT})/RT$ as below:[1,53,54]

$$\frac{\mu_w^H - \mu_w^{MT}}{RT} = -\sum_i \nu_i' \ln\left(1 + \sum_j C_{ij} f_j\right) = \sum_i \ln\left(1 + \sum_j C_{ij} f_j\right)^{-\nu_i'} \tag{3}$$

where ν_i' is the number of cavities of type i per water molecule in a unit hydrate cell, C_{ij} stands for the Langmuir constant for hydrate former's interaction with each type cavity, and f_j is the fugacity of the hydrate former.

The fugacity of water in the empty lattice can be expressed as:[1,53,54]

$$f_w^{MT} = p_w^{MT} \varphi_w^{MT} \exp \int_{p_w^{MT}}^{p} \left(\frac{\nu_w^{MT} dp}{RT}\right) \tag{4}$$

where p_w^{MT}, φ_w^{MT}, and ν_w^{MT} are the vapor pressure of the empty hydrate lattice, the correction for the deviation of the saturated vapor of the pure (hypothetical) lattice from ideal behavior, and the partial molar volume of water in the empty hydrate, respectively. The exponential term is a Poynting type correction.

Equation 4 may be simplified by two assumptions:[1,53,54]

1 that the hydrate partial molar volume is equal to the molar volume and is independent of pressure;

Table 4. Type and Concentration of Inhibitor in Aqueous Solution That Can Yield (2 and 5) K Hydrate Suppression Temperatures

inhibitor	mI1[a]	mI2[b]
methanol	0.047	0.104
ethane-1,2-diol	0.066	0.171
sodium chloride	0.047	0.108
potassium chloride	0.06	0.141
calcium dichloride	0.058	0.115

[a] Mass fraction of inhibitor in aqueous solution that can yield a 2 K hydrate suppression temperature. [b] Mass fraction of inhibitor in aqueous solution that can yield a 5 K hydrate suppression temperature.

2 that p_w^{MT} is relatively small (on the order of 10^{-3} MPa), so that $\varphi_w^{MT} = 1$.

Therefore,

$$f_w^{MT} = p_w^{MT} \exp \frac{\nu_w^{MT}(p - p_w^{MT})}{RT} \tag{5}$$

Using the previous expressions, the fugacity of water in the hydrate phase is given by:

$$f_w^H = p_w^{MT} \exp \frac{\nu_w^{MT}(p - p_w^{MT})}{RT} [(1 + C_{small} f^g)^{-\nu'_{small}} (1 + C_{large} f^g)^{-\nu'_{large}}] \tag{6}$$

where f^g is the fugacity of gaseous hydrate former in the gas phase and subscripts small and large refer to small and large cavities, respectively. The fugacity of water in the liquid water phase can be expressed by:

$$f_w^L = x_w^L \gamma_w p_w^{sat} \exp\left(\frac{\nu_w^L (p - p_w^{sat})}{RT}\right) \tag{7}$$

where x_w^L, γ_w, p_w^{sat}, and ν_w^L represent the mole fraction of water in the aqueous phase, activity coefficient of water, water vapor pressure, and molar volume of liquid water, respectively. The Krichevsky−Kasarnovsky equation[56−58] can be applied for calculation of solubility of carbon dioxide and methane in the aqueous phase as follows:

$$x_i^L = \frac{f^g}{H_{i-w} \exp\left(\frac{\nu_i^L}{RT}(p - p_w^{sat})\right)} \tag{8}$$

In eq 8, subscript i stands for either CO_2 or CH_4, $H_{i\text{-}w}$ denotes the Henry's constant of the hydrate former in water, and ν_i^L is the

Table 5. Values of the Model Parameters and the Obtained Results Using the Proposed Thermodynamic Model for Representation of the Hydrate Dissociation Conditions in the CO_2 + Ionic Liquid Aqueous Solution System[a]

$T^{Expt}_{(smoothed)}$[b]/K	CC_1[c]	CC_2[c]	CC_3[c]	A_{12}[d]	A_{21}[d]	α[d]	x_w	γ_w	f^g/MPa	$p^{Expt}_{(smoothed)}$[e]/MPa	p^{Calf}/MPa	ARD[g] %
275	0.705	−0.315	1.890	5.00	2.01	0.60	1.000	1.0000	1.193	1.466	1.518	3.5
276	0.705	−0.315	1.890	5.00	2.01	0.60	1.000	1.0000	1.313	1.668	1.725	3.4
277	0.705	−0.315	1.890	5.00	2.01	0.60	1.000	1.0000	1.439	1.897	1.961	3.4
278	0.705	−0.315	1.890	5.00	2.01	0.60	1.000	1.0000	1.566	2.156	2.228	3.3
279	0.705	−0.315	1.890	5.00	2.01	0.60	1.000	1.0000	1.693	2.449	2.530	3.3
280	0.705	−0.315	1.890	5.00	2.01	0.60	1.000	1.0000	1.815	2.781	2.873	3.3
281	0.705	−0.315	1.890	5.00	2.01	0.60	1.000	1.0000	1.923	3.157	3.262	3.3
282	0.705	−0.315	1.890	5.00	2.01	0.60	1.000	1.0000	2.004	3.582	3.704	3.4
283	0.705	−0.315	1.890	5.00	2.01	0.60	1.000	1.0000	2.027	4.062	4.212	3.7
274	0.705	−0.315	1.890	5.00	2.01	0.60	0.981	1.0147	1.263	1.618	1.647	1.8
275	0.705	−0.315	1.890	5.00	2.01	0.60	0.981	1.0165	1.391	1.857	1.885	1.5
276	0.705	−0.315	1.890	5.00	2.01	0.60	0.981	1.0183	1.522	2.129	2.155	1.2
277	0.705	−0.315	1.890	5.00	2.01	0.60	0.981	1.0199	1.653	2.440	2.465	1.0
278	0.705	−0.315	1.890	5.00	2.01	0.60	0.981	1.0214	1.778	2.795	2.818	0.8
279	0.705	−0.315	1.890	5.00	2.01	0.60	0.981	1.0224	1.888	3.200	3.223	0.7
280	0.705	−0.315	1.890	5.00	2.01	0.60	0.981	1.0226	1.966	3.663	3.689	0.7
281	0.705	−0.315	1.890	5.00	2.01	0.60	0.981	1.0211	1.960	4.189	4.240	1.2
282	0.705	−0.315	1.890	5.00	2.01	0.60	0.981	1.0010	0.402	4.790	4.860	1.5
273	0.705	−0.315	1.890	5.00	2.01	0.60	0.948	1.0201	0.4194	1.932	1.964	1.7
274	0.705	−0.315	1.890	5.00	2.01	0.60	0.948	1.0220	1.5429	2.203	2.235	1.5
275	0.705	−0.315	1.890	5.00	2.01	0.60	0.948	1.0237	1.6644	2.510	2.544	1.4
276	0.705	−0.315	1.890	5.00	2.01	0.60	0.948	1.0250	1.7779	2.861	2.898	1.3
277	0.705	−0.315	1.890	5.00	2.01	0.60	0.948	1.0258	1.8731	3.261	3.303	1.3
278	0.705	−0.315	1.890	5.00	2.01	0.60	0.948	1.0256	1.9287	3.717	3.772	1.5
279	0.705	−0.315	1.890	5.00	2.01	0.60	0.948	1.0233	1.8814	4.180	4.421	5.8
Overall												2.2

[a] The experimental data have been smoothed. [b] Smoothed experimental temperature. [c] The Mathias−Copeman[71] parameters for the PR-EoS.[60] [d] The interaction parameters of the NRTL[59] model. [e] Smoothed experimental pressure. [f] Calculated pressure. [g] ARD = $100\cdot(|p^{cal} - p^{Expt}|)/p^{Expt}$.

partial molar volume of the hydrate former. The NRTL[59] and the PR-EoS[60] have been applied for the determination of the activity coefficient of water in the aqueous phase and the fugacity of hydrate former in the gas phase, respectively.

Using previous equations, the following expression is obtained for calculating the dissociation conditions of clathrate hydrates for liquid water−hydrate−gas/vapor equilibrium:

$$x_w^L \gamma_w p_w^{sat} \exp\left(\frac{v_w^L (p - p_w^{sat})}{RT}\right) = p_w{}^{MT} \exp\frac{v_w^{MT}(p - p_w^{MT})}{RT}[(1 + C_{small} f^g)^{-\nu'_{small}}(1 + C_{large} f^g)^{-\nu'_{large}}] \quad (9)$$

Equation 9 allows easy calculation of the hydrate dissociation pressures of the investigated systems.

Model Parameters. In the preceding equations, the following values of ν_i' for sI clathrate hydrates can be used:[1,53,54,61,62]

$$\nu'_{small} = 1/23 \quad \text{and} \quad \nu'_{large} = 3/23 \quad (10)$$

The values of partial molar volume of water in the empty hydrate ($v_w{}^{MT}$) and molar volume of liquid water ($v_w{}^{L}$) are considered as 0.022655 $m^3\cdot kmol^{-1}$ and 0.018 $m^3\cdot kmol^{-1}$, respectively. Careful experimental studies[57,58] show that the most reliable values of V_i^L to estimate the solubilities of carbon dioxide and methane in water by the Krichevsky-Kasarnovsky equation[56−58] are equal to (33.9 and 34) $cm^3\cdot mol^{-1}$, respectively. The Langmuir constants were reported by Parrish and Prausnitz[63] for a range of temperatures and hydrate formers. However, the integration procedure was followed in obtaining the Langmuir constants for wider temperatures using the Kihara[1,64,65] potential function with a spherical core according to the study by McKoy and Sinanoğlu.[65] In this work, the Langmuir constants for hydrate former's interaction with each type cavity have been determined using the equations of Parrish and Prausnitz:[53,54,63] for pentagonal dodecahedra (small cavity):

$$C_{small} = \frac{a}{T}\exp\left(\frac{b}{T}\right) \quad (11a)$$

for tetrakaidecahedra (large cavity):

$$C_{large} = \frac{c}{T}\exp\left(\frac{d}{T}\right) \quad (11b)$$

where T is in K and C has unit of reciprocal MPa. The values of the constants a to d were reported by Parrish and Prausnitz.[63]

These values for methane hydrate are: a = 0.0037237 $K\cdot MPa^{-1}$, b = 2708.8 K, c = 0.018373 $K\cdot MPa^{-1}$, d = 2737.9 K; and for

dx.doi.org/10.1021/je200462q |J. Chem. Eng. Data 2011, 56, 3620–3629

Table 6. Values of the Model Parameters and the Obtained Results Using the Proposed Thermodynamic Model for the Prediction of the Hydrate Dissociation Conditions in the Methane + Ionic Liquid Aqueous Solution System[a]

$T^{Expt}_{(smoothed)}$[b]/K	CC_1[c]	CC_2[c]	CC_3[c]	A_{12}[d]	A_{21}[d]	α[d]	x_w	γ_w	f[g]/MPa	$p^{Expt}_{(smoothed)}$[e]/MPa	p^{Pred}[f]/MPa	ARD[g] %
277	0.416	−0.173	0.348	5.00	2.01	0.60	1.000	1.0000	2.985	3.813	3.822	0.2
278	0.416	−0.173	0.348	5.00	2.01	0.60	1.000	1.0000	3.244	4.259	4.256	0.1
279	0.416	−0.173	0.348	5.00	2.01	0.60	1.000	1.0000	3.516	4.756	4.736	0.4
280	0.416	−0.173	0.348	5.00	2.01	0.60	1.000	1.0000	3.801	5.308	5.268	0.7
281	0.416	−0.173	0.348	5.00	2.01	0.60	1.000	1.0000	4.097	5.922	5.858	1.1
282	0.416	−0.173	0.348	5.00	2.01	0.60	1.000	1.0000	4.403	6.604	6.510	1.4
283	0.416	−0.173	0.348	5.00	2.01	0.60	1.000	1.0000	4.717	7.362	7.230	1.8
284	0.416	−0.173	0.348	5.00	2.01	0.60	1.000	1.0000	5.038	8.204	8.026	2.2
285	0.416	−0.173	0.348	5.00	2.01	0.60	1.000	1.0000	5.363	9.139	8.904	2.6
286	0.416	−0.173	0.348	5.00	2.01	0.60	1.000	1.0000	5.693	10.176	9.870	3.0
287	0.416	−0.173	0.348	5.00	2.01	0.60	1.000	1.0000	6.026	11.327	10.931	3.5
288	0.416	−0.173	0.348	5.00	2.01	0.60	1.000	1.0000	6.363	12.603	12.096	4.0
289	0.416	−0.173	0.348	5.00	2.01	0.60	1.000	1.0000	6.708	14.019	13.369	4.6
274	0.416	−0.173	0.348	5.00	2.01	0.60	0.981	1.0001	2.778	3.539	3.516	0.6
275	0.416	−0.173	0.348	5.00	2.01	0.60	0.981	1.0001	3.019	3.946	3.910	0.9
276	0.416	−0.173	0.348	5.00	2.01	0.60	0.981	1.0001	3.274	4.399	4.347	1.2
277	0.416	−0.173	0.348	5.00	2.01	0.60	0.981	1.0001	3.541	4.905	4.832	1.5
278	0.416	−0.173	0.348	5.00	2.01	0.60	0.981	1.0001	3.821	5.469	5.372	1.8
279	0.416	−0.173	0.348	5.00	2.01	0.60	0.981	1.0001	4.112	6.098	5.970	2.1
280	0.416	−0.173	0.348	5.00	2.01	0.60	0.981	1.0001	4.413	6.798	6.635	2.4
281	0.416	−0.173	0.348	5.00	2.01	0.60	0.981	1.0001	4.721	7.580	7.372	2.7
282	0.416	−0.173	0.348	5.00	2.01	0.60	0.981	1.0001	5.035	8.451	8.188	3.1
283	0.416	−0.173	0.348	5.00	2.01	0.60	0.981	1.0001	5.354	9.422	9.093	3.5
284	0.416	−0.173	0.348	5.00	2.01	0.60	0.981	1.0001	5.676	10.505	10.092	3.9
285	0.416	−0.173	0.348	5.00	2.01	0.60	0.981	1.0001	6.001	11.713	11.196	4.4
286	0.416	−0.173	0.348	5.00	2.01	0.60	0.981	1.0001	6.331	13.059	12.412	5.0
287	0.416	−0.173	0.348	5.00	2.01	0.60	0.981	1.0001	6.669	14.560	13.747	5.6
288	0.416	−0.173	0.348	5.00	2.01	0.60	0.981	1.0001	7.020	16.234	15.209	6.3
273	0.416	−0.173	0.348	5.00	2.01	0.60	0.948	1.0009	2.973	3.865	3.861	0.1
274	0.416	−0.173	0.348	5.00	2.01	0.60	0.948	1.0009	3.264	4.396	4.368	0.6
275	0.416	−0.173	0.348	5.00	2.01	0.60	0.948	1.0009	3.569	4.998	4.940	1.2
276	0.416	−0.173	0.348	5.00	2.01	0.60	0.948	1.0009	3.888	5.679	5.583	1.7
277	0.416	−0.173	0.348	5.00	2.01	0.60	0.948	1.0009	4.217	6.451	6.308	2.2
278	0.416	−0.173	0.348	5.00	2.01	0.60	0.948	1.0009	4.555	7.324	7.122	2.8
279	0.416	−0.173	0.348	5.00	2.01	0.60	0.948	1.0009	4.896	8.311	8.036	3.3
280	0.416	−0.173	0.348	5.00	2.01	0.60	0.948	1.0009	5.239	9.428	9.062	3.9
281	0.416	−0.173	0.348	5.00	2.01	0.60	0.948	1.0009	5.581	10.689	10.210	4.5
282	0.416	−0.173	0.348	5.00	2.01	0.60	0.948	1.0009	5.922	12.114	11.491	5.1
283	0.416	−0.173	0.348	5.00	2.01	0.60	0.948	1.0009	6.266	13.722	12.916	5.9
284	0.416	−0.173	0.348	5.00	2.01	0.60	0.948	1.0009	6.619	15.538	14.495	6.7
285	0.416	−0.173	0.348	5.00	2.01	0.60	0.948	1.0009	6.990	17.585	16.235	7.7
Overall												2.8

[a] The experimental data have been smoothed. [b] Smoothed experimental temperature. [c] The Mathias−Copeman[71] parameters for the PR-EoS.[60] [d] The interaction parameters of the NRTL[59] model. [e] Smoothed experimental pressure. [f] Predicted pressure. [g] ARD = $100 \cdot (|p^{pred.} - p^{Expt}|)/p^{Expt}$.

CO2 hydrate are: a = 0.0011978 K·MPa^{-1}, b = 2860.5 K, c = 0.008507 K·MPa^{-1}, and d = 3277.9 K.

The following values for Henry's constant of hydrate former-water can be used in the Krichevsky-Kasarnovsky[56−58] equation: [53,54,61,62]

$$H_{i-w}/\mathrm{MPa} = \left(10^{A + B(T/K)^{-1} + \bar{C}\log(T/K) + D\cdot T/K}\right)\cdot 0.1 \quad (12)$$

where T and $H_{g,w}(T)$ are in K and MPa, respectively. The constants A to D for methane are: A = 147.788, B / K = -5768.3 K, C / K^{-1} = −52.2952, D/ K^{-1} = 0.018616; and for CO_2, these constants are: A = 21.6215, B / K = −1499.8 K, C / K^{-1} = −5.64947, D/ K^{-1} = 0.0002062.

By equating the fugacity of water in the hydrate phase to that of pure ice at the three-phase line, Dharmawardhana et al.[66] obtained the following equation for the vapor pressure of the

dx.doi.org/10.1021/je200462q |J. Chem. Eng. Data 2011, 56, 3620–3629

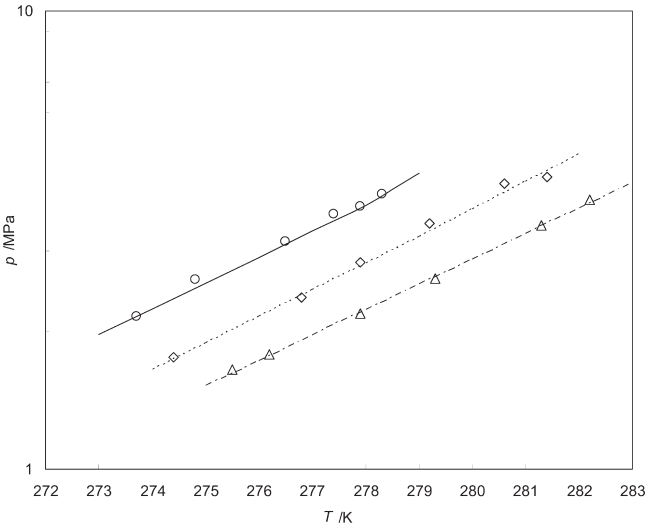

Figure 4. Calculated results using the proposed model for dissociation conditions of clathrate hydrates in the CO_2 + $[3C_4C_1P][MeSO_4]$ + water systems. p = pressure; T = temperature. Symbols represent experimental data, and curves (lines) represent the model results; △, CO_2 + water system, this work; ◇, CO_2 + IL + water system (0.2611 mass fraction IL), this work; ○, CO_2 + IL + water system (0.5007 mass fraction IL), this work; dash−dotted curve: calculated results for the CO_2 + water system, round dot curve: calculated results for the CO_2 + IL + water system (0.2611 mass fraction IL), solid curve: calculated results for the CO_2 + IL + water system (0.5007 mass fraction IL).

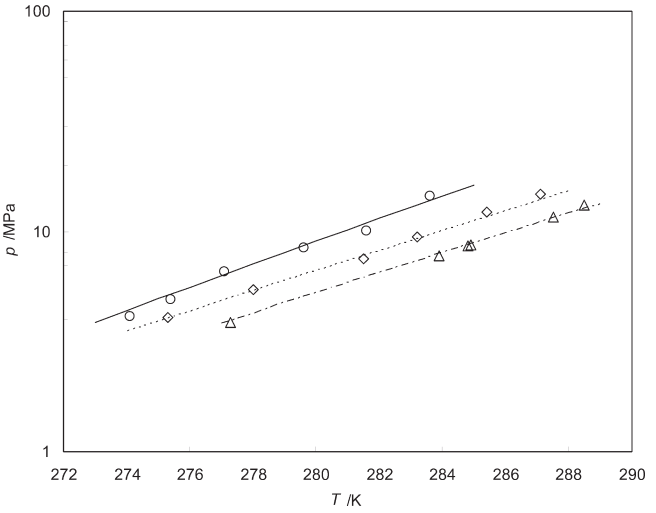

Figure 5. Calculated results using the proposed model for dissociation conditions of clathrate hydrates in the methane + $[3C_4C_1P][MeSO_4]$ + water systems. p = pressure; T = temperature. Symbols represent experimental data, and curves (lines) represent the model results; △, methane + water system, this work; ◇, methane + IL + water system (0.2611 mass fraction IL), this work; ○, methane + IL + water system (0.5007 mass fraction IL), this work. Dash−dotted curve: predicted results for the CO_2 + water system, round dot curve: predicted results for the CO_2 + IL + water system (0.2611 mass fraction IL), solid curve: predicted results for the CO_2 + IL + water system (0.5007 mass fraction IL).

empty hydrate structure I:

$$p_w^{MT}/\text{MPa} = 0.1 \exp\left(17.440 - \frac{6003.9}{T/\text{K}}\right) \quad (13)$$

where P_w^{MT} is in MPa and T is in K. The water vapor pressure can be evaluated using the following expression:[67]

$$p_w^{sat}/\text{MPa} = 10^{-6} \exp(73.649 - 7258.2/T - 7.3037 \ln(T/\text{K}) + (4.1653)(10^{-6})(T/\text{K})^2) \quad (14)$$

where T and p_w^{sat} are, respectively, in Kelvin and MPa. The parameters of the NRTL[59] and the PR-EoS[60] are calculated as explained in the next section. It should be noted that our model is based on the assumption that the investigated IL is not encapsulated in the hydrate cages. However, this fact requires rigorous confirmation using suitable techniques like Raman spectroscopy, nuclear magnetic resonance (NMR), or X-ray diffraction (XRD). On the other hand, it is evident that this assumption is not true for the systems including semiclathrate hydrates, for example, in the hydrate former + TBAB, TBAC, TBAF, and so forth aqueous solution systems because it has been demonstrated that the halide ions take part in the structure of the water cages and the TBA^- ions are encapsulated in these cages with different structures than in the traditional clathrate hydrates.[35−40]

4. RESULTS AND DISCUSSION

All of the measured hydrate dissociation data are reported in Table 2 and plotted in Figures 2 and 3. A semilogarithmic scale has been used in these figures to show the data consistency, as the logarithm of hydrate dissociation pressure versus temperature has approximately linear behavior.[1] In these figures, we have also shown some selected experimental data from the literature on the dissociation conditions of carbon dioxide and methane clathrate hydrates in the presence of pure water.[68,69] As can be seen, the agreement between our experimental data and those reported in the literature is quite good, demonstrating the reliability of the experimental method used in our work.[28,29,50−52] It is inferred from Figures 2 and 3 that the aqueous solutions of tributylmethylphosphonium methylsulfate have thermodynamic inhibition effects on clathrate hydrates of carbon dioxide and methane. It should be noted that the inhibition effect contributes to the shifting of the hydrate dissociation conditions to higher pressures/lower temperatures due to the presence of an IL in the aqueous solution. This hydrate inhibition effect on carbon dioxide and methane hydrates is, indeed, dependent on the (molar) concentration of the IL in the aqueous solution and is independent of the type of clathrate hydrate former. For instance, the hydrate suppression temperatures of approximately (2 and 5) K are obtained for 0.2611 and 0.5007 mass fractions of the IL in the aqueous solutions, respectively, for both carbon dioxide and methane clathrate hydrates. The hydrate suppression temperature is defined as the difference between hydrate dissociation temperature in the presence (T) and absence of inhibitors (T_0):[70]

$$T = T_0 - \Delta T \quad (15)$$

where ΔT is the hydrate suppression temperature (or suppression of hydrate dissociation temperature). It is of interest to compare the inhibition effect of this IL with other common hydrate inhibitors. For this purpose, ΔT can be calculated using

the following equation:[70]

$$\Delta T/\mathrm{K} = [C_1'(w_1 \cdot 100) + C_2'(w_1 \cdot 100)^2 + C_3'(w_1 \cdot 100)^3] \cdot [C_4' \ln(p/\mathrm{kPa}) + C_5'] \cdot [C_6'((p_0 - 1000)/\mathrm{kPa}) + 1] \quad (16)$$

where w_1, p, and p_0 are mass fraction of the inhibitor in the aqueous phase and pressures of the system and dissociation pressure of fluid in the presence of pure water at 273.15 K. The constants C_i' are reported in Table 3 for common hydrate inhibitors.[70] It should be mentioned that the reliability of the predictions through the aforementioned equation has already been demonstrated.[70]

Using eq 16, we can determine the concentrations of various inhibitors in aqueous solutions required to yield approximately (2 and 5) K hydrate suppression temperatures. Table 4 summarizes the type of inhibitor and its concentration in the aqueous solutions required to yield the aforementioned values of hydrate suppression temperatures. As can be seen, the inhibition effect of the aforementioned IL is not comparable to traditional hydrate inhibitors as high concentrations of this IL are required, in comparison with other common hydrate inhibitors, to yield approximately (2 and 5) K hydrate suppression temperatures.

To develop a thermodynamic model for predicting equilibrium conditions, the Mathias−Copeman[71] alpha function has been applied to determine the fugacity of CO_2/methane in vapor/gas phase assuming the latter phase is free from any water content. The binary interaction parameters of the NRTL[59] model have been tuned using the hydrate dissociation conditions for the CO_2 + IL aqueous solution system and later applied for prediction of the activity coefficient of water in the methane + IL aqueous solution system. The optimum values of the model parameters and the represented/predicted results are reported in Tables 5 and 6. Figures 4 and 5 show the determined dissociation conditions using the proposed thermodynamic model. To obtain these results, the experimental data have been smoothed using the most accurate exponential function. Acceptable agreement of the represented/predicted results in comparison with the experimental values indicates the reliability of the developed model. The results of the proposed model may be even improved through optimization of the parameters of eqs 11a and 11b against experimental dissociation pressure values.

As discussed before, the gas hydrate formation phenomenon has been already proposed for the separation of ILs from aqueous solutions.[48] It is argued in this work that such a separation process in the case of the investigated IL may need high operational pressure conditions due to the inhibition effect of tributylmethylphosphonium methylsulfate. Therefore, there is a need to apply "water-insoluble" promoters, for example, cyclopentane and cyclohexane, in the corresponding separation process to decrease/increase the pressure/temperature of hydrate formation conditions. However, this point merits future experimental investigations.

5. CONCLUSIONS

In this study, experimental hydrate dissociation data were reported for the carbon dioxide + tributylmethylphosphonium methylsulfate + water and methane + tributylmethylphosphonium methylsulfate + water systems (Table 2). The concentrations of tributylmethylphosphonium methylsulfate in the aqueous solutions were 0, 0.2611, and 0.5007 mass fractions. An isochoric pressure-search method[28,29,50−52] was applied to perform the measurements. It was shown that tributylmethylphosphonium methylsulfate has an inhibition effect on the clathrate hydrates of carbon dioxide and methane in the concentration ranges studied in this work. The inhibition effect of the aforementioned IL is not comparable to common hydrate inhibitors; however, future studies of different classes of ILs (in the light of molar concentration) might yield more promising results. A thermodynamic model based on van der Waals−Platteeuw solid solution[55] theory accompanied with the PR-EoS[60] and the NRTL[59] activity model was proposed to determine the required model parameters and acceptable agreement with experimental data was found. For development of the model, it was assumed that the investigated IL does not take part in corresponding hydrate structures. It was also inferred that, because of the inhibition effect of the investigated IL, there is a need to add hydrate formation promoters to the system for the separation of the IL from aqueous solution through gas hydrate formation technology.

AUTHOR INFORMATION

Corresponding Author

*E-mail: amir-hossein.mohammadi@mines-paristech.fr. Tel.: + (33) 1 64 69 49 70. Fax: + (33) 1 64 69 49 68.

Funding Sources

This work is based upon research supported by the South African Research Chairs Initiative of the Department of Science and Technology and National Research Foundation.

ACKNOWLEDGMENT

Thokozani Ngema is acknowledged for his help in preparation of the schematic diagram. A.E. wishes to thank MINES ParisTech for providing him a Ph.D. scholarship.

REFERENCES

(1) Sloan, E. D.; Koh, C. A. *Clathrate Hydrates of Natural Gases*, 3rd ed.; CRC Press, Taylor & Francis Group: Boca Raton, FL, 2008.

(2) Akiya, T.; Shimazaki, T.; Oowa, M.; Nakaiwa, M.; Nakane, T. Hakuta, T.; Matsuo, M.; Yoshida, M. *Phase equilibria of some alternative refrigerants hydrates and their mixtures using for cool storage materials.* Proceedings of the Thirty-second Intersociety Energy Conversion Engineering Conference, Honolulu, HI, Jul 27-Aug 1, 1997; American Institute of Chemical Engineers: New York; Vol. 3, pp 1652−1655.

(3) Akiya, T.; Shimazaki, T.; Oowa, M.; Matsuo, M.; Yoshida, Y. Formation conditions of clathrates between HFC alternative refrigerants and water. *Int. J. Thermophys.* **1999**, *20*, 1753–1763.

(4) Isobe, F.; Mori, Y. H. Formation of gas hydrate or ice by direct-contact evaporation of CFC alternatives. *Int. J. Refrig.* **1992**, *15*, 137–142.

(5) Mori, T.; Mori, Y. H. Characterization of gas hydrate formation in direct-contact cool storage process. *Int. J. Refrig.* **1989**, *12*, 259–265.

(6) Zeng, L.; Guo, K.; Zhao, Y.; Shu, B.; Zhao, J. Phase equilibrium calculation for refrigerant simple gas hydrates. *Cheng Je Wu Li Hsueh Pao/J. Eng. Thermophys.* **2000**, *21/1*.

(7) Zeng, L.; Guo, K.; Zhao, Y.; Shu, B. Phase equilibrium calculation for binary refrigerant gas hydrates. *Kung Cheng Je Wu Li Hsueh Pao/J. Eng. Thermophys.* **2000**, *21/3*.

(8) Seo, Y.; Tajima, H.; Yamasaki, A.; Takeya, S.; Ebinuma, T.; Kiyono, F. A new method for separating HFC-134a from gas mixtures using clathrate hydrate formation. *Environ. Sci. Technol.* **2004**, *38*, 4635–4639.

(9) Oowa, M.; Nakaiwa, M.; Akiya, T.; Fukuura, H.; Suzuki, K.; Ohsuka, M. *Formation of CFC alternative R134a gas hydrate*. Proceedings of the Intersociety Energy Conversion Engineering Conference, 2002; Vol. 4, pp 269−274.

(10) Liang, D.; Wang, R.; Guo, K.; Fan, S. Prediction of refrigerant gas hydrates formation conditions. *J. Therm. Sci.* **2001**, *10*, 64–68.

(11) Chun, M. K.; Lee, H.; Ryu, B. J. Phase equilibria of R22 ($CHClF_2$) hydrate systems in the presence of NaCl, KCl, and $MgCl_2$. *J. Chem. Eng. Data* **2000**, *45*, 1150–1153.

(12) Chun, M. K.; Lee, H. Phase equilibria of R22 CHClF hydrate system in the presence of sucrose, glucose and lactic acid. *Fluid Phase Equilib.* **1998**, *150*−*151*, 361–370.

(13) Hashimoto, S.; Miyauchi, H.; Inoue, Y.; Ohgaki, K. Thermodynamic and Raman Spectroscopic studies on difluoromethane (HFC-32) water binary system. *J. Chem. Eng. Data* **2010**, *55*, 2764–2768.

(14) Mohammadi, A. H.; Richon, D. *Pressure*−*Temperature phase diagrams of clathrate hydrates of HFC-134a, HFC-152a and HFC-32*. AIChE Annual Meeting, Salt Lake City, UT, Nov 7−12, 2010.

(15) Guo, K.-H.; Shu, B.-F.; Meng, Z.-X.; Zeng, L. *Direct-contact gas hydrate cool storage vessel and cool storage air-conditioning system*. Chinese Patent No. ZL95107268.4, 1995.

(16) Guo, K.-H.; Shu, B.-F.; Yang, W.-J. *Advances and applications of gas hydrate thermal energy storage technology*. Proceedings of 1st Trabzon Int. Energy and Environment Symposium, Trabzon, Turkey, 1996; Vol. 1, pp 381−386.

(17) Guo, K.-H.; Shu, B.-F.; Zhang, Y. Transient behavior of energy charge−discharge and solid−liquid phase change in mixed gas-hydrate formation. In *Heat Transfer Science and Technology*; Wang, B. X., Ed.; Higher Education Press: Beijing, China, 1996; pp 728−733.

(18) Javanmardi, J.; Moshfeghian, M. Energy consumption and economic evaluation of water desalination by hydrate phenomenon. *Appl. Therm. Eng.* **2003**, *23*, 845–857.

(19) Briggs, F. A.; Hu, Y. C.; Barduhn, A. J. *New Agents for Use in the Hydrate Process for Demineralizing Sea Water*, Research and Development Progress Report No. 59; United States Department of the Interior: Washington, DC, March 1962.

(20) Huang, C. P.; Fennema, O.; Powrie, W. D. Gas hydrates in aqueous-organic systems: I. Preliminary studies. *Cryobiology* **1965**, *2*, 109–115.

(21) Huang, C. P.; Fennema, O.; Powrie, W. D. Gas hydrates in aqueous-organic systems: II. Concentration by gas hydrate formation. *Cryobiology* **1966**, *2*, 240–245.

(22) Kang, S. P.; Lee, H. Recovery of CO_2 from flue gas using gas hydrate: thermodynamic verification through phase equilibrium measurements. *Environ. Sci. Technol.* **2000**, *34*, 4397–4400.

(23) Seo, Y.; Kang, S. P. Enhancing CO_2 separation for pre-combustion capture with hydrate formation in silica gel pore structure. *Chem. Eng. J.* **2010**, *161*, 308–312.

(24) Kim, S. M.; Lee, J. D.; Lee, H. J.; Lee, E. K.; Kim, Y. Gas hydrate formation method to capture the carbon dioxide for pre-combustion process in IGCC plant. *Int. J. Hydrogen Energy* **2011**, *36*, 1115–1121.

(25) Khokhar, A. A.; Gudmundsson, J. S.; Sloan, E. D., Jr. Gas storage in structure H hydrates. *Fluid Phase Equilib.* **1998**, *150*−*151*, 383–392.

(26) Kanda, H.; Uchida, K.; Nakamura, K.; Suzuki, T. *Economics and energy requirements on natural gas ocean transportation in form of natural gas hydrate (NGH) pellets*. Proceedings of Fifth International Conference on Gas Hydrate, Trondheim, Norway, 2005; pp 1275−1282.

(27) Eslamimanesh, A.; Mohammadi, A. H.; Richon, D. An improved Clapeyron model for predicting liquid water-hydrate-liquid hydrate former phase equilibria. *Chem. Eng. Sci.* **2011**, *66*, 1759–1764.

(28) Belandria, V.; Eslamimanesh, A.; Mohammadi, A. H.; Théveneau, P.; Legendre, H.; Richon, D. Compositional analysis and hydrate dissociation conditions measurements for carbon dioxide + methane + water system. *Ind. Eng. Chem. Res.* **2011**, *50*, 5783–5794.

(29) Belandria, V.; Eslamimanesh, A.; Mohammadi, A. H.; Richon, D. Gas hydrate formation in carbon dioxide + nitrogen + water system: Compositional analysis of equilibrium phases. *Ind. Eng. Chem. Res.* **2011**, *50*, 4722–4730.

(30) Belandria, V.; Eslamimanesh, A.; Mohammadi, A. H.; Richon, D. Study of gas hydrate formation in the carbon dioxide + hydrogen + water systems: Compositional analysis of the gas phase. *Ind. Eng. Chem. Res.* **2011**, *50*, 6455–6459.

(31) Mainusch, S.; Peters, C. J.; de Swaan Arons, J.; Javanmardi, J.; Moshfeghian, M. Experimental determination and modeling of methane hydrates in mixtures of acetone and water. *J. Chem. Eng. Data* **1997**, *42*, 948–950.

(32) Jager, M. D.; de Deugd, R. M.; Peters, C. J.; de Swaan Arons, J.; Sloan, E. D. Experimental determination and modeling of structure II hydrates in mixtures of methane + water + 1,4-dioxane. *Fluid Phase Equilib.* **1999**, *165*, 209–223.

(33) de Deugd, R. M.; Jager, M. D.; de Swaan Arons, J. Mixed hydrates of methane and water-soluble hydrocarbons modeling of empirical results. *AIChE J.* **2001**, *47*, 693–704.

(34) Ng, H. J.; Robinson, D. B. New developments in the measurement and prediction of hydrate formation for processing needs. *Ann. N. Y. Acad. Sci.* **1994**, *715*, 450–462.

(35) Li, S.; Fan, S.; Wang, J.; Lang, X.; Wang, Y. Semiclathrate hydrate phase equilibria for CO_2 in the presence of tetra-n-butyl ammonium halide (bromide, chloride, or fluoride). *J. Chem. Eng. Data* **2010**, *55*, 3212–3215.

(36) Makino, T.; Yamamoto, T.; Nagata, K.; Sakamoto, H.; Hashimoto, S.; Sugahara, T.; Ohgaki, K. Thermodynamic stabilities of tetra-n-butyl ammonium chloride + H_2, N_2, CH_4, CO_2, or C_2H_6 semiclathrate hydrate systems. *J. Chem. Eng. Data* **2010**, *55*, 839–841.

(37) Mayoufi, N.; Dalmazzone, D.; Fürst, W.; Delahaye, A.; Fournaison, L. CO_2 enclathration in hydrates of peralkyl-(ammonium/phosphonium) salts: Stability conditions and dissociation enthalpies. *J. Chem. Eng. Data* **2010**, *55*, 1271–1275.

(38) Deschamps, J.; Dalmazzone, D. Hydrogen storage in semiclathrate hydrates of tetrabutyl ammonium chloride and tetrabutyl phosphonium bromide. *J. Chem. Eng. Data* **2010**, *55*, 3395–3399.

(39) Lee, S.; Lee, Y.; Park, S.; Seo, Y. Phase equilibria of semiclathrate hydrate for nitrogen in the presence of tetra-*n*-butylammonium bromide and fluoride. *J. Chem. Eng. Data* **2010**, *55*, 5883–5886.

(40) Mohammadi, A. H.; Richon, D. Phase equilibria of semiclathrate hydrates of tetra-*n*-butylammonium bromide + hydrogen sulfide and tetra-*n*-butylammonium bromide + methane. *J. Chem. Eng. Data* **2010**, *55*, 982–984.

(41) Welton, T. Room-temperature ionic liquids. Solvents for synthesis and catalysis. *Chem. Rev.* **1999**, *99*/ *8*, 2071–2084.

(42) Marsh, K. N.; Deev, A.; Wu, A. C. T.; Tran, E.; Klamt, A. Room temperature ionic liquids as replacements for conventional solvents − A review. *Korean J. Chem. Eng.* **2002**, *19*/*3*, 357–362.

(43) Eslamimanesh, A.; Gharagheizi, F.; Mohammadi, A. H.; Richon, D. Artificial neural network modeling of solubility of supercritical carbon dioxide in 24 commonly used ionic liquids. *Chem. Eng. Sci.* **2011**, *66*, 3039–3044.

(44) Chen, Q.; Yu, Y.; Zeng, P.; Yang, W.; Liang, Q.; Peng, X.; Liu, Y.; Hu, Y. Effect of 1-butyl-3-methylimidazolium tetrafluoroborate on the formation rate of CO_2 hydrate. *J. Nat. Gas Chem.* **2008**, *17*, 264–267.

(45) Xiao, C.; Adidharma, H. Dual function inhibitors for methane hydrate. *Chem. Eng. Sci.* **2009**, *64*, 1522–1527.

(46) Xiao, C.; Wibisono, N.; Adidharma, H. Dialkylimidazolium halide ionic liquids as dual function inhibitors for methane hydrate. *Chem. Eng. Sci.* **2010**, *65*, 3080–3087.

(47) Li, X.-S.; Liu, Y.-J.; Zeng, Z.-Y.; Chen, Z.-Y.; Li, G.; Wu, H.-J. Equilibrium Hydrate Formation Conditions for the Mixtures of Methane + Ionic Liquids + Water. *J. Chem. Eng. Data* **2011**, *56*, 119–123.

(48) Peng, X.; Hu, Y.; Liu, Y.; Jin, C.; Lin, H. Separation of ionic liquids from dilute aqueous solutions using the method based on CO_2 hydrates. *J. Nat. Gas Chem.* **2010**, *19*, 81–85.

(49) Letcher, T. M.; Reddy, P. Determination of activity coefficients at infinite dilution of organic solutes in the ionic liquid, tributylmethylphosphonium methylsulphate by gas−liquid chromatography. *Fluid Phase Equilib.* **2007**, *260*, 23–28.

(50) Tohidi, B.; Burgass, R. W.; Danesh, A.; Østergaard, K. K.; Todd, A. C. Improving the Accuracy of Gas Hydrate Dissociation Point Measurements. *Ann. N.Y. Acad. Sci.* **2000**, *912*, 924–931.

(51) Ohmura, R.; Takeya, S.; Uchida, T.; Ebinuma, T. Clathrate hydrate formed with methane and 2-Propanol: Confirmation of structure II hydrate formation. *Ind. Eng. Chem. Res.* **2004**, *43*, 4964–4966.

(52) Afzal, W.; Mohammadi, A. H.; Richon, D. Experimental measurements and predictions of dissociation conditions for carbon dioxide and methane hydrates in the presence of triethylene glycol aqueous solutions. *J. Chem. Eng. Data* **2007**, *52*, 2053–2055.

(53) Mohammadi, A. H.; Richon, D. Development of predictive techniques for estimating liquid water-hydrate equilibrium of water-hydrocarbon system. *J. Thermodynamics.* **2009**, 1–12.

(54) Mohammadi, A. H.; Richon, D. Thermodynamic model for predicting liquid water-hydrate equilibrium of the water-hydrocarbon system. *Ind. Eng. Chem. Res.* **2008**, *47*, 1346–1350.

(55) van der Waals, J. H.; Platteeuw, J. C. Clathrate solutions. *Adv. Chem. Phys.* **1959**, *2*, 1–57.

(56) Krichevsky, I. R.; Kasarnovsky, J. S. Thermodynamical calculations of solubilities of nitrogen and hydrogen in water at high pressures. *J. Am. Chem. Soc.* **1935**, *57*, 2168–2172.

(57) Ruffine, L.; Trusler, J. P. M. Phase behaviour of mixed-gas hydrate systems containing carbon dioxide. *J. Chem. Thermodyn.* **2010**, *42*, 605–611.

(58) Dhima, A.; de Hemptinne, J.; Jose, J. Solubility of hydrocarbons and CO_2 mixtures in water under high pressure. *Ind. Eng. Chem. Res.* **1999**, *38*, 3144–3161.

(59) Renon, H.; Prausnitz, J. M. Liquid-liquid and vapor-liquid equilibria for binary and ternary systems with dibutyl ketone, dimethyl sulfoxide, n-hexane, and 1-hexene. *Ind. Eng. Chem. Process Des. Dev.* **1968**, *7*, 220–225.

(60) Peng, D. Y.; Robinson, D. B. A new two-constant equation of state. *Ind. Eng. Chem. Fundam.* **1976**, *15*, 59–64.

(61) Eslamimanesh, A.; Mohammadi, A. H.; Richon, D. Thermodynamic consistency test for experimental data of water content of methane. *AIChE J.* **2010**, DOI 10.1002/aic.12462.

(62) Eslamimanesh, A.; Mohammadi, A. H.; Richon, D. Thermodynamic consistency test for experimental solubility data in carbon dioxide/methane + water system inside and outside gas hydrate formation region. *J. Chem. Eng. Data* **2011**, *56*, 1573–1586.

(63) Parrish, W. R.; Prausnitz, J. M. Dissociation pressures of gas hydrate formed by gas mixture. *Ind. Eng. Chem. Process Des. Dev.* **1972**, *11*, 26–34.

(64) Kihara, T. Virial coefficient and models of molecules in gases. *Rev. Mod. Phys.* **1953**, *25*, 831–843.

(65) McKoy, V.; Sinanoğlu, O. Theory of dissociation pressures of some gas hydrates. *J. Chem. Phys.* **1963**, *38*, 2946–2956.

(66) Dharmawardhana, P. B.; Parrish, W. R.; Sloan, E. D. Experimental thermodynamic parameters for the prediction of natural gas hydrate dissociation conditions. *Ind. Eng. Chem. Fundam.* **1980**, *19*, 410–414.

(67) Daubert, T. E.; Danner, R. P. *DIPPR Data Compilation Tables of Properties of Pure Compounds*, AIChE: New York, NY, 1985.

(68) Fan, S. S.; Chen, G. J.; Ma, Q. L.; Guo, T. M. Experimental and modeling studies on the hydrate formation of CO_2 and CO_2-rich gas mixtures. *Chem. Eng. J.* **2000**, *78*, 173–178.

(69) Nakamura, T.; Makino, T.; Sugahara, T.; Ohgaki, K. Stability boundaries of gas hydrates helped by methane - structure-H hydrates of methylcyclohexane and cis-1,2-dimethylcyclohexane. *Chem. Eng. Sci.* **2003**, *58*, 269–273.

(70) Østergaard, K. K.; Masoudi, R.; Tohidi, B.; Danesh, A.; Todd, A. C. A general correlation for predicting the suppression of hydrate dissociation temperature in the presence of thermodynamic inhibitors. *J. Pet. Sci. Eng.* **2005**, *48*, 70–80.

(71) Mathias, P. M.; Copeman, T. W. Extension of the Peng-Robinson equation-of-state to complex mixtures: Evaluation of the various forms of the local composition concept. *Fluid Phase Equilib.* **1983**, *13*, 91–108.